

Redshifts and Optical Properties for a Statistically Complete Sample of Poor Galaxy Clusters

Michael J. Ledlow, Chris Loken, Jack O. Burns
New Mexico State University, Dept. of Astronomy, Box 30001/Dept. 4500,
Las Cruces, NM 88003-0001

John M. Hill
Steward Observatory, University of Arizona, Tuscon, AZ 85721

and

Richard A. White
NASA/Goddard Space Flight Ctr., Space Data and Computing Division, Code 932, Greenbelt,
MD 20771

ABSTRACT

From the poor cluster catalog of White *et al.* (1996), we define a sample of 71 optically- selected poor galaxy clusters. The surface-density enhancement we require for our clusters falls between that of the loose associations of Turner and Gott (1976) and the Hickson compact groups (Hickson, 1982). We review the selection biases and determine the statistical completeness of the sample. For this sample, we report new velocity measurements made with the ARC 3.5-m Dual-Imaging spectrograph and the 2.3-m Steward Observatory MX fiber spectrograph. Combining our own measurements with those from the literature, we examine the velocity distributions, velocity dispersions, and 1-d velocity substructure for our poor cluster sample, and compare our results to other poor cluster samples. We find that approximately half of the sample may have significant 1-d velocity substructure. The optical morphology, large-scale environment, and velocity field of many of these clusters are indicative of young, dynamically evolving systems. In future papers, we will use this sample to derive the poor cluster X-ray luminosity function and gas mass function, and will examine the optical/X-ray properties of the clusters in more detail.

1. Introduction

Galaxy groups or poor clusters are interesting for many reasons. Poor clusters are much more numerous than rich clusters like those in the Abell (1958) catalog. One estimate suggests that over 50% of all galaxies reside in a poor cluster environment (Dressler, 1984; Soneira & Peebles, 1978). Because of their high space density, poor clusters are very good tracers of large-scale structure, and hence, their properties may provide important constraints to cosmological models of large-scale formation.

The definition of a poor cluster is rather vague. In most respects, *poor* simply means that the number of galaxies falls below some limiting (for instance Abell’s richness class 0) criteria for a *rich* cluster. In practice, there are many existing catalogs of poor clusters which each differ greatly in their selection criteria, such as the degree of isolation, compactness, and galaxy counts. Some of the earlier poor cluster catalogs (Shakhbazyan, 1973; Rose, 1977; Hickson, 1982) concentrated on very compact systems, with surface-density enhancements as high as 100-1000 times that of the mean field density (*e.g.* Hickson Compact Groups (HCG)). Many of these compact groups have surface densities equal to or greater than the centers of many rich clusters. Conversely, Turner and Gott (1976) defined a catalog of poor clusters, using a friends-of-friends approach, which located many *loose* systems with only a 4.6 surface-density enhancement over the field. Other selection criteria, such as the presence of a dominant cD or D-type first-ranked galaxy (Albert, White, & Morgan, 1977; Morgan, Kayser, & White, 1975) have resulted in other poor cluster samples (the AWM and MKW clusters). Thus, *poor clusters* can span the entire range from isolated pairs of galaxies to just below the threshold of rich galaxy clusters. It is for this reason that poor clusters are so valuable for studies of galaxy formation, dynamics, and evolution, as well as hierarchical large-scale structure formation and cosmology.

The optical properties of various poor cluster samples have been studied recently by Beers *et al.* (1995) (MKW and AWM clusters), Diaferio, Geller, & Ramella (1994) (HCG), Dell’Antonio, Geller, & Fabricant (1994) (MKW, AWM, and White *et al.* 1996 clusters), and Ramella *et al.* (1994) (HCG’s and CfA loose groups). The existence of very compact groups is particularly troublesome because of their short crossing times ($t_{cr} \leq 0.02 H_0^{-1}$) (Diaferio, Geller, & Ramella 1994). Dynamical friction should cause the galaxies to merge into a single system on a time-scale of order 5-10 crossing times (the merging instability, *e.g.* Barnes 1985). Thus, it is surprising that we see any very compact groups at all. If the merging scenario does occur in compact groups, the AWM and MKW clusters may be good candidates for the end-result, culminating in the formation of a very extended central-dominant galaxy. Beers *et al.* used this idea to look for D/cD galaxies in MKW and AWM clusters with large peculiar velocities relative to the cluster mean in order to constrain dynamical ages and merging time-scales. They found 4/29 clusters with possibly significant D/cD velocity offsets which may be in the process of forming the dominant galaxy via the merger of member galaxies. The lifetime problem may be resolved, however, if compact systems are continually forming within collapsing, rich, loose clusters (Ramella *et al.* 1994). Beers *et al.* Ramella *et al.* and Diaferio *et al.* all show evidence that compact groups are often imbedded

within, and often gravitationally bound to much larger galaxy associations. There is substantial evidence to suggest that loose/compact groups may be related by similar formation mechanisms or via an evolutionary sequence from loose to compact systems. Thus, dynamical studies of large samples of poor groups are very important to better our understanding of how clusters form and evolve.

What is the relationship between poor and rich clusters? X-ray studies have shown that most poor groups are in fact real galaxy associations with a detectable hot intragalactic medium (IGM) with $T \sim 1$ keV (*e.g.* Doe *et al.* 1995). Relationships between the X-ray luminosity, temperature and optical measures, such as the velocity dispersion, suggest that poor clusters are simply lower mass extensions of richer clusters (Price *et al.* 1991). However, there appears to be a turnover in the L_x vs. σ_v relationship as the member galaxies contribute a larger and larger fraction of the total X-ray emission (Dell’Antonio, Geller, & Fabricant 1994). This relationship is also complicated because the velocity dispersion is not necessarily a good estimator of the mass of the system if the cluster is not relaxed (Diaferio, Geller, & Ramella 1995). Additionally, there is some evidence to suggest that the distribution of dark matter, the baryon fraction, and mass-to-light ratios may be different from rich clusters (Dell’Antonio, Geller, & Fabricant 1995; David, Jones, & Forman 1995). These conclusions are fairly controversial, however, because data of sufficient quality are only available for a few clusters. In order to address these questions, one needs large samples. It is with these goals in mind that we have defined a new sample of poor clusters for a detailed study of their optical, x-ray, and radio properties, and their connection to existing statistical samples of rich clusters.

We describe the selection of the poor cluster sample in section 2. In section 3, we present the observations and the new velocity measurements for this sample. In section 4, we examine the completeness of the sample, and select a volume-limited subsample for further study. In section 5, we discuss the velocity distributions, dispersions, and the results of statistical 1-D normality tests. We discuss the properties of several clusters in detail in the appendix.

Throughout this paper we assume $H_0 = 75$ km sec⁻¹ Mpc⁻¹ and $q_0 = 0.5$.

2. Sample Selection

The galaxy clusters were selected from the electronic version of the Zwicky catalog of galaxies and clusters of galaxies (CGCG) (Zwicky *et al.* 1961-1968). White *et al.* (1996) used a friends-of-friends technique (Turner and Gott 1976) to identify galaxy groups based on surface-density enhancements relative to the north galactic polar cap and included all galaxies to the magnitude limit of the survey (15.7). The catalog was searched in 10° galactic latitude strips with a 1° overlap with successive scans in order to avoid missing groups near the edge of the strips. The base-level surface density enhancement of the entire catalog is 21.54 (or 100^{2/3}, equal to a volume-density enhancement of 100) with a minimum of 3 Zwicky galaxies per group. This search

produced > 600 potential groups, including all MKW, AWM, WP (White 1978) groups as well as some nearby Abell clusters (Abell 1958). Radio observations of a subsample of this catalog were reported in Burns *et al.* (1987). An X-ray/optical study of groups from the Burns *et al.* sample with *Einstein* observations was reported in Price *et al.* (1991).

In this paper, and those to follow in this series, we have constructed a statistically complete subsample of the original White *et al.* catalog corresponding to those groups with a 46.4 surface-density enhancement (a $10^{1/3}$ higher volume density over the base-level of the catalog), which included 4 or more Zwicky galaxies, and with galactic latitude $|b| \geq 30^\circ$. After eliminating several Abell clusters (A119, A194, A400, A634, A779, A1185, A1213, A1367, A1656, A1983, A2022, the Hercules and Pisces superclusters, A2052, A2063, A2199, A2634, and A2666) and 4 redundant groups (those found in more than one search strip) the sample contains 71 poor clusters. Statistically, approximately 39% of the poor clusters have only the minimum number of 4 galaxies down to the magnitude limit of the search. The distribution of galaxy number has a tail which extends to a maximum of 10, with a mean of 6 galaxies. The entire poor cluster sample is listed in Table 1.

3. Observations

A thorough search of the literature and the NED extragalactic database revealed that only about half of the sample had > 2 measured velocities per cluster. We require a minimum of 2 concordant velocities in order to reliably determine the distance to the cluster. We therefore began a program to measure recessional velocities for the remainder of these clusters in order to use this sample to study the statistical properties of nearby poor clusters.

Spectroscopic observations of the cluster galaxies were obtained using the Astrophysical Research Consortium’s (ARC) 3.5-meter telescope at Apache Point, NM. The instrument used was the Dual-Imaging Spectrograph (DIS) mounted at the Nasmyth focus. The DIS allows both imaging and spectroscopy modes by rotating either mirrors or gratings, mounted in a turret wheel, into the light path. Two grating sets are available; a low-resolution set (150/300 lines mm^{-1}) with $6\text{-}7\text{\AA}$ pixel^{-1} spectral resolution, and a high-resolution set (831/1200 lines mm^{-1}) at $1\text{-}1.7\text{\AA}$ pixel^{-1} . All observations reported here were made in low-resolution mode.

The incoming light-beam is split by a dichroic filter with a wavelength cutoff near 5700\AA . The blue and red beams are each directed along separate light-paths to two CCD detectors. The blue-chip is a TEK 512x512 CCD, and the red-chip a TI 800x800 array. Plate-scales are $1.086''/\text{pixel}$ and $0.61''/\text{pixel}$ on the blue and red chips, respectively. The field-of-view on both chips is approximately $6' \times 4'$. A filter wheel is mounted behind the dichroic with a Gunn g,r set for imaging mode. The spectra are also obtained separately from the blue and red chips. In low-resolution mode, the spectral coverage extends from $3800 - 10000\text{\AA}$, divided into two parts blueward and redward of 5700\AA . A separate filter wheel is located at the focal-plane at the

entrance to the spectrograph to hold the slit for spectroscopy.

We report observations made on the nights of 27-28 November 1994, 24-25 January, 9 March, and 22 May 1995. On the earlier observing runs, we used a single 2'' slit, and rotated the detector to align two or more galaxies along the slit. In later runs, we used custom-designed slit masks in order to observe 4-12 galaxies simultaneously. Candidate galaxies were identified from images extracted from the CD-ROM Digital POSS I Survey. Positions were measured with $< 1''$ accuracy, and pointing centers were determined by optimizing the maximum number of galaxies which could be fit into the DIS field-of-view. From these coordinate files, an aperture slit-mask was designed matching the imaging scale of the DIS spectrograph using a custom-written IDL program. By default, we used $18'' \times 2''$ slits oriented East-West. In some cases, slits were located off-center from the galaxy position in order to observe galaxies closer than $18''$ separation in right-ascension. The final versions of the slit-masks are saved to a Postscript file and printed on Kodak infrared film on a 2500 dpi typesetter as a negative transparency. Tests have shown the negative transparency film to be very opaque (no scattered light problems), and the clear slits to have approximately equal transmission as compared to the default Quartz-slits used in the DIS. These slit-masks are cut out and placed in the filter/slit-wheel at the entrance to the spectrograph.

The observing procedure consisted of 1) imaging the poor cluster field through the Gunn g,r filters in imaging mode, 2) imaging the slit-mask to locate the positions of the slits on the detector, 3) using an on-line Fortran program to calculate the necessary right-ascension and declination offsets and rotation angle in order to align the candidate galaxies in the appropriate slits, 4) offsetting the telescope and rotating the instrument as determined in (3), and 5) moving the gratings into the light-path and beginning the exposure. Typical exposure times were 10 minutes. Wavelength calibration was obtained by taking spectra of Helium-Neon calibration lamps following each object observation.

We used standard spectroscopic reduction procedures in IRAF to analyze the spectra. The bias-level was determined from a 30 column overscan region, and a zero-frame was subtracted to remove large-scale bias fluctuations. For the single-slit observations, a spectral flatfield was used to correct for the illumination pattern of the slit and cosmetic defects on the CCD chips. For the multislit data, spectral flats were complicated by overlapping dispersion patterns from adjacent slits (using the continuum lamp), so this correction was not used. For single-slit observations, the wavelength solution was determined for both axes of the 2-d image. For the multislit data, the wavelength solution was applied to the background-subtracted and extracted 1-d spectra. This was necessary as each spectrum had a unique wavelength range dependent on the north-south position of the slit on the chip. Heliocentric radial velocities were measured using the cross-correlation program FXCOR. We observed several nearby galaxies and G and K-type radial velocity standard stars as template spectra for the cross-correlations. For the R-spectra, the atmospheric A-band was removed by restricting the wavelength range for the cross-correlation for both the object and template.

In Figure 1, we show a sample ARC 3.5-m DIS spectrum for IC 4508 in the poor group N67-310 at a redshift of $z = 0.045$. IC 4508 is one of 7 galaxies observed for this cluster using the slit masks discussed above. In Figure 1(a) we show the blue portion of the spectrum from $3800 - 5700 \text{ \AA}$. The red portion of the spectrum in Figure 1(b) extends from $\sim 5700 - 10500 \text{ \AA}$. The shape of the spectrum redward of 5250 \AA on the blue spectra, and blueward of 6100 \AA on the red spectra is due to the wavelength cutoff of the dichroic.

In addition to the ARC 3.5-m observations, we also report multifiber spectroscopic observations of 3 poor clusters from this statistical sample and 3 other poor clusters from the larger sample of Burns *et al.* (1987) with ROSAT PSPC observations reported in Doe *et al.* (1995) plus one other cluster (N03-183) which meets the statistical sample definition, but is located at low galactic latitude (23°). These data were obtained in January and July 1994 using the University of Arizona’s Steward Observatory 2.3-m telescope and the MX multifiber spectrograph. A detailed description of the design and construction of the MX spectrometer is given by Hill and Lesser (1986). The detector was a UV-flooded Loral 1200×800 pixel CCD with a read-noise of 8 electrons pixel^{-1} rms. A 400 line mm^{-1} grating provided wavelength coverage from 3700 to 6950 \AA at 8 \AA resolution ($2.8 \text{ \AA pixel}^{-1}$).

In Table 2, we list the new ARC heliocentric velocity measurements for our poor cluster sample. We have identified the individual galaxies from positions measured from the Digital-Sky Survey and cross-correlated with NED and the Zwicky catalog. Some identifications from these catalogs corresponded to galaxy pairs with a single name. In these cases, we have used the catalogued designation and appended a number to distinguish the objects. Hubble types for the galaxies were determined from examination of the Gunn g,r images from DIS. Table 3 lists heliocentric velocities measured using MX for the clusters S49-128, S34-111, S49-140, S49-132, N56-394, MKW2, and N03-183.

4. Sample Properties

In order to use this sample of galaxy clusters for statistical studies and, in particular, for determination of the X-ray luminosity function (Burns *et al.* 1996), it is necessary to examine the completeness in terms of a volume-limited sample. In Figure 2, we plot the volume density of clusters as a function of redshift. We see that for $z > 0.03$, the volume density begins to fall off rapidly. This is a well-known consequence of the magnitude limit of the Zwicky catalog. As one goes to higher redshift, the number of group galaxies with magnitudes brighter than 15.7 decreases because of the shape of the optical luminosity function. Thus at higher redshift, we are only able to pick out clusters with higher richness values and more bright galaxies. These clusters may therefore not be representative of the sample below $z = 0.03$. Below redshifts of $z = 0.01$, there are only 4 clusters in the catalog, and these are most likely members of the Local Group. We eliminated these clusters from the statistical sample because the measured velocities may be strongly affected by peculiar motions. Within the Poisson counting errors of our

sample (49 clusters with $0.01 \leq z \leq 0.03$), there is no statistical difference between the observed volume-density and a flat distribution with a mean of $2.9 \pm 0.3 \times 10^{-5} \text{ Mpc}^{-3}$. We therefore judge our sample volume-limited within observational uncertainties. In Table 1, we have marked those clusters which fall outside our volume-limited sample with an asterisk. Our statistical sample includes 49 poor clusters. We calculate that our survey covers 10973 square degrees (3.34 steradians) or 26.6% of the sky.

The base-level catalog from White *et al.* includes clusters selected from all galactic latitude strips, limited only by the -3° declination cutoff of the Zwicky catalog. In the selection of this sample, we have limited the galactic latitude range to $|b| \geq 30^\circ$. We investigated whether some incompleteness in the sample could be attributed to galactic absorption at the lower latitudes. Within the error bars, the surface density of clusters is constant as a function of galactic latitude.

What is the relationship between our poor clusters and Zwicky clusters? Zwicky did not use a strict definition (as did Abell) for defining clusters. In fact, his catalog contains clusters with a wide range in properties. His open clusters are very large structures ($\geq 1^\circ$) which may contain many smaller subclumps of galaxy groups. Surface-density enhancements were also cataloged as either medium compact or compact. We performed a cross-correlation between our 67 (excluding the 4 clusters with $z < 0.01$) poor clusters and the nearby Zwicky clusters. We find that 53/67 are found within catalogued clusters. Another 6 are not within the Zwicky cluster boundary, but are near a cluster, or in a group of clusters. Eight do not appear to be associated with any listed Zwicky cluster. Of the 53 which were found in Zwicky clusters, 26 are classified as open, 26 as medium compact, and 1 as compact. Four of the poor clusters are located within the Coma supercluster, and one within the Hercules supercluster. Also, some of Zwicky’s clusters contain more than one of our poor clusters (*e.g.* N56-359, N56-371, N56-392 all in Zw1141.7–0158, N34-169 and N45-388 in Zw0909.7+1814). The location of our poor clusters within Zwicky’s contours is variable, ranging from centrally located to the edge of the galaxy distribution (see Doe *et al.* 1995).

We compared the 26:26:1 compactness ratio for our sample to the nearby Zwicky clusters in general. From Zwicky’s catalog, 504 clusters are classified as nearby from apparent magnitudes or velocity information. The ratio of Open:Medium-Compact:Compact is 274:205:25. From a 2×2 contingency table test there is no statistically significant difference in the ratios between our sample and the nearby Zwicky catalog. Thus our sample appears to be representative of Zwicky clusters in general. It is interesting that nearly half of our sample is located within Zwicky’s open clusters. The statistics described above also suggest that a large fraction of our clusters are correlated with or are embedded within larger-scale structures. We will examine this question with regard to the velocity field and velocity dispersions in the next section.

5. Velocity Distributions and Dispersions

Of the 71 clusters listed in Table 1, 40 have ≥ 5 velocity measurements within a 0.5 Mpc projected radius from the optical center of the cluster. We report velocity dispersions for all clusters with ≥ 5 measurements in column 6. We have calculated the Biweight estimators of location and scale (C_{BI} and S_{BI}) (Beers, Flynn, & Gebhardt 1990) rather than the average and standard deviation (Danese, DeZotti, & di Tullio 1980). These quantities are less sensitive to small number statistics and outliers in the velocity distribution. In addition, we list the 1σ confidence intervals determined from the Jackknife method (Mosteller & Tukey 1977). For those clusters which had at least a 50% increase in the number of velocities out to 1 Mpc, we also list the velocity dispersion separately for $R \leq 1$ Mpc in column 8.

In Figure 3, we plot a histogram of the velocity dispersions measured within 0.5 Mpc. The median dispersion is 295 ± 31 km sec $^{-1}$ (using the error on the median). Approximately 17% of the clusters fall in the tail of the distribution, with $\sigma_v > 500$ km sec $^{-1}$. Zabludoff, Huchra, & Geller (1990) reported an average $\sigma_v = 744$ km sec $^{-1}$ for a sample of nearby rich clusters. Thus, there is a small amount of overlap in the long-tail of our distribution with richer clusters. Ramella *et al.* (1994) compared the velocity dispersions of 29 HCG’s to 36 loose systems (RGH) selected from the CfA redshift survey. They calculated median values of 329 ± 135 and 403 ± 96 for the HCG and RGH clusters, respectively. For 21 MKW and AWM clusters, Beers *et al.* (1995) found a median dispersion of 336 ± 40 km sec $^{-1}$. These values are consistent with our sample, although it should be noted that both Ramella *et al.* and Beers *et al.* included galaxies out to a larger radius (1.125 Mpc for $H_0 = 75$).

Diaferio *et al.* (1994) computed velocity dispersions for a number of simulated compact groups using an N-body Treecode (Hernquist, 1987; Barnes & Hut 1986). They found a median $\sigma_v = 257$ km sec $^{-1}$ for their simulated clusters. While this is lower than our value of 295 km sec $^{-1}$, given the large spread in our distribution, the results may be consistent. Our observed distribution has $\sim 17\%$ more clusters with $S_{BI} \geq 400$ km sec $^{-1}$ than predicted by the simulations. However, given the errors on the velocity dispersions, it is unlikely that this result is statistically significant. We performed a KS-test and T-test to compare the S_{BI} distribution in Figure 3 to the simulated data from Diaferio *et al.* (Figure 8(a) in their paper). We can reject the hypothesis that the two distributions are drawn from the same parent population at no better than the 20% level.

We have compared the velocity dispersions for $r \leq 0.5$ Mpc, $r \leq 1$ Mpc, and 0.5 Mpc $\leq r \leq 1$ Mpc. Because of the often low number of velocities, the errors on the dispersions are quite large. We find that a histogram of the difference in S_{BI} for different radii is consistent with a Gaussian spread of values with FWHM ~ 200 km sec $^{-1}$. The best-fit Gaussian is slightly skewed towards higher S_{BI} ($\Delta S_{BI} \sim 75$ km sec $^{-1}$). Within the errorbars, however, the significance of the difference from zero is inconclusive. Ramella *et al.* (1994) claimed that in general, the velocity dispersion increases when one includes the larger association around HCG’s. Such analysis has the potential of providing important dynamical information on poor clusters,

but large numbers of velocities are needed.

In Figure 4, we show velocity histograms for the 23 clusters with ≥ 10 measurements from Table 1, as well as the four additional clusters listed in Table 3 (S49-132, N03-183, S49-128, & MKW 2). With the exception of MKW 2, all plots are scaled to $C_{BI} \pm 2000 \text{ km sec}^{-1}$ to allow easy comparison of the dispersions between different clusters. We have used the ROSTAT package (Beers, Flynn, & Gebhardt 1990) to estimate measures of the normality of the velocity histograms with respect to a Gaussian distribution. In dissipationless systems, dynamical evolution will be dominated by gravity. N-body models show that over a relaxation time, galaxy-galaxy interactions will distribute the velocities in a Gaussian distribution. Thus, we might expect that significant departures from a Gaussian may be indicative of a non-equilibrium or non-virial dynamical state. Ideally, however, one needs large numbers of velocities, and powerful 2-D and 3-D tests to understand the true dynamical state of a cluster (see Pinkney *et al.* 1996). Velocity information is also limited to line-of-sight measurements, so the results are not unambiguous depending on the three dimensional spatial distribution of the galaxies (*i.e.* our viewing angle). The results, however, may be illuminating with regards to the amount of velocity substructure present in our sample.

These statistical tests are very robust with respect to Poisson noise and low number statistics, however, erroneous results can be found due to outliers in the velocity distribution. We have used the 3σ -clipping criteria as prescribed by Yahil & Vidal (1977) to eliminate possible interlopers. The inclusion of non-cluster members is particularly troublesome for poor clusters because of the typically low number of member galaxies. Even a few outliers can severely bias the velocity dispersion and other scaling parameters. In addition to the standard tests performed by ROSTAT (U-test, W-test, B_1 -test, B_2 -test, $B_1 - B_2$ omni-test, I-test, KS-stat, V-stat, W^2 -stat, U^2 -stat, U-stat, and A^2 -stat), we also evaluate the Tail-index (TI) and Asymmetry-Index (AI) described in Bird & Beers (1993) (see Beers *et al.* 1990, and Pinkney *et al.* 1996 and references therein for a complete description of these tests). All of these statistics are sensitive to either skewness or kurtosis (the third and fourth moments of the velocity distribution), and as such are useful measures of departures from a true Gaussian distribution. Pinkney *et al.* (1996) has shown that the B_1 and AI-stat are the most powerful discriminators of skewness. The W-test and TI-stat are the most sensitive to kurtosis. Many of the other tests do not separate these two effects, but are useful for comparing the importance of one or the other effect as the cause of the non-normality.

Even after 3σ clipping, 55% (15/27) of the clusters show significant non-normality ($\geq 90\%$ significance) in at least one of the statistics, which we regard as a conservative lower limit of the fraction of poor clusters in our sample with complex velocity distributions. For these clusters we have plotted velocity-coded spatial (RA vs. DEC) diagrams in Figure 5. These plots are useful for locating 3-D substructure and galaxy clumps imbedded within the galaxy distribution. In most cases, however, the velocity structure in the clusters is quite complicated. It is clear that in all 15 cases there is no strong velocity/spatial segregation with respect to the center or outskirts of the cluster. This result is not specific to these 15 clusters, but appears to be true in general for

our sample. To quantify the 3-D nature of these clusters, we have also used a modified version of the Dressler-Shectman statistic (DS) (Dressler & Shectman, 1988) to look for 3-d substructure. Because of the small number of total galaxies in these clusters, we have used a modified version of the DS-test to use a window including the \sqrt{N} nearest neighbors rather than 10 as suggested in the original test (Pinkney *et al.* 1996). We describe the results of the 1-D and DS statistics individually for all 15 clusters in the appendix.

As discussed in the previous section, 88% of our sample is located within or near a catalogued Zwicky cluster. We have compared the velocity dispersions for the clusters divided by the open/medium-compact classification, and those not found within Zwicky’s contours (isolated). We used the S_{BI} (≤ 0.5 Mpc) values listed in Table 1. The median S_{BI} are: isolated, 205 ± 66 km sec⁻¹; located within open clusters, 290 ± 47 ; and medium-compact clusters, 329 ± 51 (quoted errors are the error on the median). Within the errors these values are probably consistent, however, it is interesting that the median values steadily increase from isolated clusters to large, loose associations to more compact structures. As described in the appendix, this situation is additionally complicated because of the location of what we define as a poor cluster within a more extended galaxy distribution. Because of the surface-density requirement in selecting our poor clusters, it seems very likely that we are simply picking out local density maxima or clumps in a much larger gravitationally bound system. Beers *et al.* (1995) examined these trends with several AWM and MKW clusters and found that many galaxy groups separated by as much as 3 Mpc in projection may be consistent with being gravitationally bound to one another (one very good example is the poor cluster pair MKW7/MKW8). Only about 12/63 of our clusters are found at the center of Zwicky’s clusters. The remainder are located throughout the galaxy association, often embedded in a larger cluster with several other high surface-density clumps.

6. Conclusions

It is clear that the dynamics of poor clusters can be very complicated. Even within the inner 1 Mpc, which we have investigated, over half of the clusters show evidence for non-equilibrium or non-virial conditions. This suggests that many of these clusters are in fact young, dynamically evolving systems, which, in many cases, are simply a part of a much larger conglomerate of galaxies.

Our poor clusters have very similar properties to other samples of poor clusters with a variety of selection criteria. The presence of dominant cluster galaxies or differences in the richness or compactness of the cluster do not significantly change the observed velocity dispersions or other optical properties.

As poor cluster samples and galaxy velocity databases grow larger, we may gain a better appreciation for the complexity of hierarchical cluster formation. We plan to use the statistical sample presented in this paper for future studies, including an examination of the galaxy

morphologies, X-ray and radio properties, and the relationship to the richness and the local dynamics.

We acknowledge J. Pinkney for his help with the statistical analysis. We thank the Steward Observatory of the University of Arizona for generous allocation of observing time. We also thank T. Beers, the referee, for providing the ROSTAT analysis package, and for a careful reading of the text. The Apache Point Observatory is maintained and operated by the Astrophysical Research Consortium (ARC). This research has made use of the NASA/IPAC Extragalactic Database (NED) which is operated by the Jet Propulsion Laboratory and the California Institute of Technology, under contract with the National Aeronautics & Space Administration. This research was supported by NSF Grant AST-9317596 to J.O.B. and C.L.

Appendix: Comments on Individual Clusters

S49-147 - The X-ray properties of this cluster are discussed in Price *et al.* (1991) and Dell’Antonio *et al.* (1994). Burns *et al.* (1987) report no radio identifications from their VLA survey. The B_1 , B_2 , $B_1 - B_2$, and TI-tests all reported significant substructure. The implied skewness, however, is caused by the one galaxy at 6359 km sec^{-1} . This galaxy survived the 3σ clipping, but is responsible for the positive result. S49-147 is located within the open cluster Zw0014.5+2315.

AWM 1 - Also called N45-388, this cluster is discussed in detail by Beers *et al.* (1995), who extend the search radius beyond 3 Mpc. They found 3 separate groups at distances between 1.9-2.7 Mpc which are consistent with being gravitationally bound to the primary cluster. Within our 1 Mpc search radius, we find mildly significant kurtosis to the right of the mean (B_2 - test). The DS-test found significant clumping to the south and north-east of the dominant central galaxy. Burns *et al.* (1987) found no radio galaxies in this cluster. AWM 1 is located near the edge of the open cluster Zw0909.7+1814, which also includes N34-169 at the center.

MKW 10 - Also called N67-312, this cluster is discussed by Beers *et al.* . In a more extended region around the cluster, they found 2 clumps at distances of 2.22 and 2.6 Mpc which may be bound to this cluster. Within the inner 1 Mpc region, the velocity dispersion is quite small, but exhibits significant non-normality (B_1 , KS , W^2 , U^2 , A^2 , and AI-test) which is attributed to skewness leftward of the mean velocity. There is one compact radio source associated with an S0 galaxy. MKW 10 is located within the medium-compact cluster Zw1138.3+1024.

N79-298B - Only the B_2 and AI-tests were significant for this cluster. This is a result of the very sharp truncation of the velocity distribution at 4300 and 4900 km sec^{-1} (tails are too short). The DS-test found significant structure, which may be partly due to the extreme elongation in the galaxy distribution. This cluster is also called WP 19 (White 1978), and is located in a region near Abell 1367 (within the Coma supercluster) in the medium-compact cluster Zw1153.0+2522.

N79-299B - The 1-D non-normality is dominated by the two galaxies between 6200-6450 km sec^{-1} which causes some degree of both skewness and kurtosis (W , B_1 , KS , W^2 , U^2 , and A^2 tests). The 3-D distribution is very clumpy. However, the velocity mean and dispersion is very similar in both clumps which resulted in a negative result for the DS-test. There are two compact radio sources associated with this cluster. This cluster is also named WP 21, and is located within Zw1202.0+2028, a large open cluster which also includes WP 20 (N79-299A, see below).

N79-299A - Only very moderate kurtosis is present in the velocity distribution because of the sharp truncation to the right of the mean, and skewness from the slight asymmetry to the left. The X-ray properties of this cluster were discussed by Doe *et al.* (1995). The spatial distribution is very elongated and clumpy, however the DS-test reported a negative result. This cluster contains three compact radio sources and a wide-angle tailed radio galaxy located at the mean cluster velocity. N79-299A (or WP 20) is found within Zw1202.0+2028, in the same large open cluster as N79-299B (WP 21).

N67-330 - This is a very nearby, spiral-rich cluster. The velocity distribution is strongly skewed, and several tests were significant (W , B_1 , B_2 , $B_1 - B_2$, W^2 , U^2 , A^2 , and U). The average significance of 6 kurtosis tests was 97% (90% for skewness).

N79-292 - The velocity distribution is strongly skewed to the right of the mean (W , B_1 , and AI tests had >95% significance). The spatial distribution is very clumpy, however, the two primary groups have similar velocity fields. The DS-test found a positive result (92%) for the two galaxies to the south-west of the cluster. N79-292 is not located within a catalogued Zwicky cluster, but is near Zw1224.1+0914 (a medium-compact cluster).

MKW 11 - Beers *et al.* found two clumps ~ 2.25 Mpc to the north with very similar velocities which are consistent with being bound to the primary cluster. Within 1 Mpc, there is significant kurtosis to the left of the mean at the 90% level (B_2 and U -tests). There are two compact radio sources in this cluster. Also called N79-296, MKW 11 is located within the open cluster Zw1327.3+1145. There is another nearby Zwicky cluster in the immediate area as well.

N79-286 - The X-ray properties of this cluster are discussed in Price *et al.* (1991). All four velocities outside the primary peak in the histogram were clipped by the 3σ -limit. The velocity dispersion is quite low (146 km sec^{-1}). The B_2 and U -tests found significant kurtosis (tails too short) with a slight skewness to the left of the mean. The 3-D distribution is very disperse with only one tight grouping near the cluster center and no apparent substructure. This cluster is also identified with HCG 68.

MKW 12 - Beers *et al.* note that this cluster is trimodal, with no significant large-scale structure outside the several groupings within the inner Mpc. All but the B_2 and $B_1 - B_2$ tests reported significant non-normality. This result is clearly due to the multimodal nature of the distribution. Within the inner 1 Mpc, the DS-test did not find significant 3-D clumping. MKW 12 is also called N67-336, and is located at the center of Zw1400.4+0949, a medium-compact cluster.

S49-132 - The X-ray and optical properties of this cluster are discussed in Doe *et al.* (1995). There are three radio galaxies within the central part of the cluster, each associated with a Zwicky galaxy (two compact sources and one tailed source). The velocity distribution is very broad, with each of the radio/Zwicky galaxies separated by greater than 1000 km sec^{-1} . The very strong X-ray emission and the presence of the tailed radio source argue against simple projection effects, however, the velocity distribution is very unusual for a poor cluster. The B_2 , U , and AI tests were significant at the 97% level (tails too short for the large velocity dispersion). The DS-test found significant 3-D structure at the 94% level. The elongation in the galaxy distribution follows the distribution of the X-ray gas. One possible interpretation is that we are viewing a cluster which is accreting galaxies along a large-scale filament. S49-132 is located within a larger galaxy isodensity contour in the middle of a compact Zwicky cluster.

N03-183 - This cluster is not part of the statistical sample in Burns *et al.* (1987) due to its low galactic latitude (25°). It does, however, meet the surface-density enhancement requirement of the sample presented in this paper. The cluster was observed as part of a backup program with

the MX. The cluster is unusual in that we detected 7 emission-line galaxies from the MX spectra. Most of the other clusters contained one or possibly two such galaxies. Positive signals were found from the W , B_1 , U , and AI-tests, indicating significant asymmetries and skewness to the left of the mean, and moderate kurtosis (tails too short). The DS-test did not find a positive signal for 3-D substructure.

S49-128 - The X-ray properties of this cluster were discussed by Doe *et al.* (1995). The cluster contains a large double or Wide-angle tailed radio source with a velocity of 6481 km sec^{-1} , near the center of the primary velocity concentration. The velocity distribution, however, is very boxy, and strongly skewed to the left with slight kurtosis to the right (short velocity tail) (B_1 , B_2 , $B_1 - B_2$, I , A^2 , and AI-tests). The single spatial outlier to the northwest falls within the 3σ -limit, so was not clipped. The distribution, however, is non-Gaussian even when this object is excluded. S49-128 is found near the north-edge of a large open Zwicky cluster.

MKW2 - This optical properties of this cluster are discussed by Beers *et al.* (1995), the X-ray and radio by Doe *et al.* (1995). The cluster contains a wide-angle tailed radio source associated with a cD galaxy with velocity $11260 \text{ km sec}^{-1}$ (within the largest peak in the velocity distribution). While the velocity distribution appears bimodal (as also noted by Beers *et al.*) between $10000 - 12000 \text{ km sec}^{-1}$, the statistical tests found only a weak non-Gaussian signature. The 3 galaxies near 9000 and one galaxy near $13000 \text{ km sec}^{-1}$ were 3σ -clipped. MKW 2 is located near the edge of a medium-compact Zwicky cluster.

REFERENCES

- Abell, G.O. 1958, ApJS, 3, 211
- Albert, C.E., White, R.A., & Morgan, W.W. 1977, ApJ, 211, 309
- Barnes, J.E. 1985, MNRAS, 215, 517
- Barnes, J.E. & Hut, P. 1986, *Nature*, 338, 123
- Beers, T.C., Flynn, K., & Gebhardt, K. 1990, AJ, 100, 32
- Beers, T.C., Kriessler, J.R., Bird, C.M., & Huchra, J.P. 1995, AJ, 109, 874
- Bird, C.M. & Beers, T.C. 1993, AJ, 105, 1596
- Bryan, G. *et al.* 1996, in preparation
- Burns, J.O. Hanisch, R.J., White, R.A., Nelson, E.R., Morrisette, K.A., & Moody, J.W. 1987, AJ 94, 587
- Burns, J.O., Ledlow, M.J., Loken, C., Klypin, A., Voges, W., Bryan, G., & Norman, M. 1996, in preparation.
- Danese, L, DeZotti, G., & di Tullio, G. 1980, A&A, 82, 322
- David, L.P., Jones, C., & Forman, W. 1995, ApJ, 445, 578

- Dell’Antonio, I.P., Geller, M.J., & Fabricant, D.G. 1994, AJ, 107, 427
- Dell’Antonio, I.P., Geller, M.J., & Fabricant, D.G. 1995, AJ, 110, 502
- Diaferio, A., Geller, M.J., & Ramella, M. 1994, AJ, 107, 868
- Diaferio, A., Geller, M.J., & Ramella, M. 1995, AJ, 109, 2293
- Doe, S.M., Ledlow, M.J., Burns, J.O., & White, R.A. 1995, AJ, 110, 46
- Dressler, A. 1984, ARA&A, 22, 185
- Dressler, A. & Schectman, S.A. 1988, AJ, 95, 985
- Hernquist, L. 1987, ApJS, 64, 715
- Hickson, P. 1982, ApJ, 255, 382
- Hill, J.M. & Lesser, M.P. 1986, in *Proceedings of SPIE Conference on Instrumentation in Astronomy VI, SPIE*, 627, 303
- Morgan, W.W., Kayser, S., & White, R.A. 1975, ApJ, 199, 545
- Mosteller, F. & Tukey, J.W. 1977, in *Data Analysis and Regression* (Addison Wesley, Reading, MA), p. 133
- Pinkney, J., Roettiger, K., Burns, J.O., & Bird, C.M. 1996, ApJS, in press
- Price, R., Burns, J.O., Duric, N., & Newberry, M.V. 1991, AJ, 102, 14
- Ramella, M., Diaferio, A., Geller, M.J., & Huchra, J.P. 1994, AJ, 107, 1623
- Rose, J.A. 1977, ApJ, 211, 311
- Shakhbazyan, R.K. 1973, *Astrofiz*, 9, 495
- Soneira, R.M. & Peebles, P.J.E. 1978, ApJ, 211, 1
- Turner, E.L. & Gott, J.R. 1976, AJ, 91, 204
- White, R.A. 1978, ApJ, 226, 591
- White, R.A., Bhavsar, S., Bornmann, P., & Burns, J.O. 1996, in preparation
- Yahil, A. & Vidal, N.V. 1977, ApJ, 214, 347
- Zabludoff, A.I., Huchra, J.P., & Geller, M.J. 1990, ApJS, 74, 1
- Zwicky, F., Herzog, E., Karpowicz, M., Kowal, C.T., & Wild, P. 1961-1968, *Catalogue of Galaxies & Clusters of Galaxies* (Caltech, Pasadena)

Table 1. Poor Cluster Sample

Cluster	RA(2000)	DEC(2000)	z	N	S_{BI}	N	S_{BI}	Ref	Other Name
				$\leq 0.5 \text{ Mpc}$	$\leq 0.5 \text{ Mpc}$	$\leq 1 \text{ Mpc}$	$\leq 1 \text{ Mpc}$		
S34-115	00 18 18.7	30 02 41	0.0225	10	474^{+168}_{-93}	12	...	NED	
S49-147	00 21 30.1	22 26 39	0.0191	8	289^{+172}_{-84}	12	233^{+141}_{-43}	NED	
S34-111	01 07 27.7	32 23 59	0.0173	29	466^{+55}_{-41}	47	486^{+53}_{-37}	MX	
S49-140	01 56 22.9	05 37 37	0.0179	10	205^{+59}_{-21}	13	...	MX	
S49-141	02 01 47.8	08 28 25	0.0264	4	...	4	...	APO	
S49-145	02 07 34.9	02 08 14	0.0227	6	519^{+41}_{-30}	7	...	NED	
S49-142	03 20 44.7	-01 02 15	0.0211	6	69^{+2}_{-2}	7	...	NED	
N45-342	09 10 10.9	50 24 47	0.0165	3	...	3	...	NED	
N34-169	09 16 11.8	17 39 28	0.0292	3	...	3	...	APO/NED	
N45-388	09 17 31.6	19 51 24	0.0291	7	584^{+238}_{-193}	20	608^{+94}_{-53}	BKBH	AWM 1
*N45-366	09 23 39.3	22 21 07	0.0316	6	888^{+226}_{-65}	6	...	APO/NED	
N45-384	09 27 51.8	29 59 56	0.0266	7	238^{+125}_{-14}	11	185^{+84}_{-40}	NED	
N34-170	09 42 24.6	04 16 16	0.0292	2	...	2	...	APO	
N34-172	10 00 32.1	-02 57 27	0.0207	8	337^{+135}_{-45}	9	...	BKBH	MKW 1
N56-393	10 13 52.0	38 40 07	0.0221	6	422^{+99}_{-24}	6	...	NED	
*N56-387	10 25 18.2	17 08 44	0.0025	3	...	3	...	NED	
*N56-367	10 27 05.5	16 04 40	0.0331	2	...	2	...	APO	
*N56-388	10 41 24.4	06 10 17	0.0310	3	...	3	...	NED	
*N45-371	11 20 12.8	72 50 35	0.0373	2	...	2	...	APO/NED	
*N56-396	11 21 28.3	02 52 33	0.0496	3	...	3	...	APO	
N67-311	11 22 26.8	24 17 33	0.0264	6	149^{+186}_{-53}	6	...	RDGH	HCG 51
N67-322	11 28 35.1	09 05 29	0.0210	6	45^{+18}_{-16}	6	...	NED	
*N56-359	11 36 21.3	-02 50 37	0.0454	2	...	2	...	APO	
*N79-278	11 37 54.4	21 58 23	0.0306	8	344^{+57}_{-14}	8	...	RDGH	HCG 57
N67-312	11 42 04.6	10 18 20	0.0206	9	177^{+85}_{-46}	11	...	BKBH	MKW 10
*N79-290	11 44 12.9	33 40 20	0.0325	4	...	5	236^{+67}_{-6}	APO/NED	
N56-371	11 45 03.5	-01 39 38	0.0276	3	...	3	...	APO/NED	
*N79-280	11 46 18.5	33 09 19	0.0325	4	...	4	...	NED	
N67-300	11 48 22.5	12 43 19	0.0129	4	...	5	446^{+226}_{-256}	RDGH	HCG 59
N56-392	11 49 38.9	-03 31 35	0.0272	8	106^{+167}_{-58}	8	...	APO/BKBH	MKW 3
N79-298	11 57 52.3	25 10 18	0.0153	12	185^{+30}_{-32}	13	...	NED	
N79-299B	12 04 09.5	20 13 18	0.0235	5	232^{+159}_{-3}	14	384^{+151}_{-110}	NED	
N67-335	12 04 21.7	01 50 19	0.0204	22	607^{+135}_{-52}	31	568^{+85}_{-70}	BKBH	MKW 4
N79-299A	12 05 51.2	20 32 19	0.0235	9	495^{+130}_{-72}	15	419^{+84}_{-49}	NED	
N79-282	12 12 25.9	29 08 20	0.0132	5	85^{+37}_{-4}	10	89^{+19}_{-11}	NED	HCG 61
N79-268	12 19 42.9	28 47 22	0.0253	4	...	4	...	NED	
N79-283	12 19 54.8	28 25 21	0.0259	2	...	2	...	APO	
*N67-330	12 20 02.3	05 20 24	0.0068	32	413^{+76}_{-40}	55	485^{+63}_{-41}	NED	
N79-292	12 24 14.7	09 20 24	0.0235	7	445^{+88}_{-13}	18	558^{+147}_{-95}	NED	
N79-284	12 35 58.4	26 58 29	0.0246	4	...	7	598^{+277}_{-69}	NED	
*N67-333	13 04 25.3	07 54 54	0.0449	2	...	2	...	APO	
N67-323	13 05 26.5	53 33 56	0.0289	4	...	4	...	APO	
N67-317	13 13 49.0	06 57 09	0.0217	2	...	2	...	APO	
N79-270	13 17 19.3	20 37 11	0.0226	4	...	4	...	NED	
N79-296	13 29 22.3	11 47 31	0.0232	8	424^{+146}_{-21}	14	384^{+70}_{-42}	BKBH	MKW 11
N67-329	13 32 36.4	07 20 36	0.0231	5	155^{+54}_{-51}	5	...	APO/NED	
N67-318	13 52 19.0	02 20 19	0.0235	2	...	2	...	APO	
*N79-286	13 53 31.0	40 16 17	0.0085	14	145^{+173}_{-18}	27	183^{+77}_{-36}	NED	HCG 68
N79-297	13 55 24.7	25 03 20	0.0293	7	178^{+103}_{-42}	7	...	RDGH	HCG 69
*N79-276	13 56 22.3	28 31 23	0.0358	3	...	3	...	NED	
N67-336	14 03 04.0	09 26 35	0.0196	18	625^{+153}_{-118}	31	721^{+176}_{-162}	BKBH	MKW 12
N67-325	14 09 58.5	17 32 51	0.0171	5	320^{+66}_{-54}	6	...	NED	

Table 1—Continued

Cluster	RA(2000)	DEC(2000)	z	N	S_{BI}	N	S_{BI}	Ref	Other Name
				$\leq 0.5 \text{ Mpc}$	$\leq 0.5 \text{ Mpc}$	$\leq 1 \text{ Mpc}$	$\leq 1 \text{ Mpc}$		
*N56-361	14 15 12.6	04 52 04	0.0559	2	...	2	...	APO/NED	
N67-326	14 28 14.1	25 50 38	0.0153	8	299^{+83}_{-41}	14	289^{+50}_{-39}	BKBH	AWM 3
N67-309	14 28 31.6	11 22 38	0.0265	6	292^{+97}_{-27}	8	...	APO/NED	
N56-394	14 34 00.9	03 44 53	0.0289	8	663^{+387}_{-440}	16	573^{+363}_{-172}	BKBH	MKW 7
N56-395	14 40 43.2	03 27 12	0.0272	7	329^{+110}_{-97}	15	422^{+99}_{-53}	BKBH	MKW 8
N56-381	14 47 00.4	11 35 29	0.0295	5	265^{+22}_{-22}	6	...	NED	
*N67-310	14 48 06.2	31 44 32	0.0453	5	111^{+28}_{-4}	5	...	APO/NED	
*N56-365	14 58 26.7	48 27 59	0.0370	2	...	2	...	APO	
*N45-381	15 13 11.6	04 28 50	0.0360	4	...	4	...	APO/NED	
N56-374	15 36 30.3	43 31 08	0.0189	5	55^{+16}_{-2}	6	...	NED	
*N45-361	15 49 36.8	42 01 56	0.0355	3	...	3	...	APO/NED	
*N45-363	15 57 46.9	16 16 27	0.0354	3	...	3	...	NED	
*N45-389	16 17 39.2	35 05 45	0.0301	9	239^{+87}_{-17}	11	...	NED	
N34-171	16 41 35.4	57 50 21	0.0176	3	...	3	...	APO	
N34-175	17 15 21.4	57 22 43	0.0283	7	589^{+440}_{-31}	APO/NED	
N34-173	17 55 24.9	62 36 40	0.0266	4	...	4	...	NED	
S49-146	22 50 17.7	11 35 53	0.0250	6	482^{+102}_{-54}	10	617^{+132}_{-110}	NED	
*S49-143	23 01 48.9	15 58 09	0.0077	8	153^{+55}_{-16}	11	136^{+37}_{-18}	NED	
S49-144	23 16 24.2	15 51 22	0.0146	2	...	2	...	NED	

References. — (BKBH) Beers, T.C. *et al.* 1995; (RDGH) Ramella, M. *et al.* 1994; (APO) This paper; (MX) This paper; (NED) Found through search of the NED Extragalactic database.

*Cluster is not part of statistical sample for $0.01 < z < 0.03$.

Table 2. ARC 3.5-m Velocity Measurements

Cluster	Galaxy	RA(2000)	DEC(2000)	V_H	Error	Hubble Type
S49-141	NGC 0791	02 01 44.32	08 30 00.1	7905	75	E
	UGC 01513	02 01 47.23	08 28 35.9	7547	100	S/I
N34-169	0915+176	09 15 56.26	17 38 33.8	9046	200	S
N45-366	UGC 04991 #1	09 23 27.17	22 19 33.6	9558	95	E
	UGC 04991 #2	09 23 25.99	22 19 01.2	9293	95	E
	UGC 04991 #3	09 23 24.18	22 18 50.4	10261	105	E
	0923+223a	09 23 31.32	22 18 30.6	9117	77	S
	*0923+223b	09 23 29.97	22 19 38.9	8219	100	E
N34-170	UGC 05182	09 42 25.04	04 16 57.2	8631	48	E
	*CGCG 035-032	09 42 13.38	04 16 25.2	8469	50	S
N56-367	CGCG 094-058	10 27 05.47	16 00 41.4	9653	89	S
	CGCG 094-062	10 27 14.74	16 02 56.8	10171	73	E
N45-371	1121+728	11 21 28.77	72 48 29.6	11194	115	S
N56-396	CGCG 039-135	11 21 32.56	02 53 13.8	14616	56	E
	NGC 3647	11 21 38.58	02 53 30.0	14714	80	E
	CGCG 039-140	11 21 35.30	02 53 37.5	15256	82	E
N56-359	CGCG 012-037	11 36 19.29	-02 50 50.1	13812	150	S
	CGCG 012-036	11 36 14.01	-02 52 13.8	13418	160	S
N79-290	*CGCG 186-029N1	11 44 03.35	33 32 06.2	9501	100	S
	CGCG 186-029N2	11 44 04.36	33 32 33.8	9230	100	S
N56-371	CGCG 012-076	11 45 15.03	-01 42 11.0	8147	87	E
	CGCG 012-074	11 45 06.38	-01 40 09.3	8220	107	S
N56-392	CGCG 012-098	11 49 39.72	-03 31 47.2	8210	120	S
	CGCG 012-095	11 49 35.44	-03 29 18.0	8215	78	E
	1149-034	11 49 32.28	-03 28 34.2	8141	80	I
N79-283	CGCG 158-074	12 19 54.80	28 23 21.2	7594	126	S
	CGCG 158-078	12 20 10.21	28 23 19.9	7912	160	E
N67-333	CGCG 043-128	13 04 14.44	07 54 13.4	13646	98	E
	CGCG 043-127	13 04 07.20	07 54 55.3	13326	140	E
N67-323	NGC 4967	13 05 36.42	53 33 51.9	8812	145	E
	MRK 0239	13 05 25.82	53 35 30.5	11331	98	E
	1305+536	13 05 19.61	53 35 39.5	15636	112	I
	1305+535	13 05 14.38	53 34 12.7	9126	150	S
	1304+536	13 04 58.64	53 36 34.5	26880	140	S
N67-317	1304+535	13 04 56.87	53 35 29.9	9405	129	E
	CGCG 044-036	13 13 55.17	06 57 07.7	6375	87	S
	CGCG 044-033	13 13 44.77	06 59 22.6	6620	140	S
N67-329	CGCG 045-011	13 32 54.65	07 19 39.4	7099	78	S
	NGC 5209	13 32 42.55	07 19 37.7	7042	74	E
	CGCG 045-008	13 32 32.31	07 17 38.9	6821	150	S
N67-318	CGCG 045-124	13 52 22.76	02 20 43.0	6981	150	S/E

Table 2—Continued

Cluster	Galaxy	RA(2000)	DEC(2000)	V_H	Error	Hubble Type
N56-361	CGCG 045-122	13 52 14.53	02 21 33.2	11149	200	E
	1415+049	14 15 16.77	04 54 28.3	16819	98	S
	CGCG 046-076	14 15 12.07	04 52 19.6	13796	150	S
N67-309	CGCG 046-073	14 14 54.24	04 54 15.7	22396	160	S
	CGCG 075-048	14 28 40.83	11 22 05.0	8184	130	S
	*CGCG 075-043	14 28 20.68	11 21 33.9	7766	100	S
	CGCG 075-044	14 28 22.43	11 25 05.0	7914	63	E
N67-310	CGCG 164-027	14 48 08.35	31 42 36.7	9888	117	E
	CGCG 164-028	14 48 07.35	31 44 16.7	13567	128	E
	IC 4508 (1)	14 47 50.77	31 45 53.2	13513	98	E
	IC 4508 (2)	14 47 47.90	31 46 51.3	13700	107	E
N56-365	*1448+317	14 48 12.89	31 44 33.2	13639		I
	CGCG 248-035	14 58 32.27	48 29 04.6	10993	75	E
N45-381	CGCG 248-034	14 58 27.76	48 29 32.6	11210	74	E
	1513+044	15 13 28.14	04 27 56.4	15964	100	S
	CGCG 049-054	15 13 18.60	04 28 38.9	11484	102	E
N45-361	CGCG 049-049	15 13 10.43	04 28 55.5	10980	85	E
	CGCG 049-045	15 13 08.24	04 29 49.3	9829	150	S
	CGCG 222-052	15 49 38.28	42 02 03.5	10076	96	E
	CGCG 049-045	15 13 08.24	04 29 49.3	9829	150	S
N34-171	NGC 6211	16 41 27.83	57 47 01.4	5248	69	E
	NGC 6213	16 41 37.22	57 48 53.8	5377	46	S
	UGC 10516	16 41 44.87	57 50 55.9	5204	78	S
N34-175	IC 1252	17 15 50.11	57 22 01.1	8996	108	S
	NPM1G+57.0229	17 15 47.08	57 18 08.0	7822	90	S
	1715+573a	17 15 29.18	57 21 00.1	8430	150	S/S0
	NGC 6346	17 15 24.26	57 19 22.5	8739	73	E
	1715+573b	17 15 16.58	57 19 47.5	7732	91	S/S0
	1715+573c	17 15 08.32	57 18 39.7	9280	63	S

* Emission-Line Redshift

Table 3. Steward Observatory 2.3-m MX Velocity Measurements

Cluster	Galaxy	RA(2000)	DEC(2000)	V_H	error
S49-132		23:10:31.81	+07:34:17.8		
	201	23:10:42.30	+07:34:04.1	13204	45
	203	23:10:40.60	+07:23:16.6	10979	51
	204	23:11:33.75	+07:31:49.6	11619	44
	208	23:11:07.85	+07:24:24.1	12149	61
	210	23:10:38.28	+07:33:54.9	12967	57
	211	23:10:37.36	+07:32:48.7	12352	38
	212	23:10:33.43	+07:32:19.5	12208	48
	215	23:10:49.98	+07:27:20.5	12757	82
	220	23:10:45.52	+07:26:14.2	11777	88
	226	23:10:20.74	+07:22:14.8	12245	40
	227	23:10:18.12	+07:32:42.2	10818	50
	228	23:09:53.38	+07:29:31.6	13752	49
	229	23:09:09.44	+07:30:26.1	11095	40
	*230	23:09:03.92	+07:31:04.3	12314	56
	231	23:09:59.04	+07:20:32.9	11734	46
	234	23:10:14.43	+07:27:09.3	13355	40
	236	23:10:20.81	+07:32:36.2	11225	38
	237	23:10:27.94	+07:32:46.1	12771	50
	238	23:10:03.08	+07:34:06.7	11241	39
	239	23:10:18.51	+07:34:17.8	13573	108
	244	23:10:09.46	+07:16:19.4	13401	45
	246	23:09:54.33	+07:22:16.5	11907	47
	250	23:10:30.43	+07:35:20.8	12651	39
	252	23:10:48.48	+07:35:12.0	12620	46
	254	23:10:58.94	+07:39:38.8	12838	41
	256	23:11:35.66	+07:44:35.0	12724	40
	262	23:10:22.39	+07:34:51.0	11852	38
	263	23:10:25.11	+07:34:42.0	11048	37
	264	23:10:26.86	+07:35:24.9	11273	48
265	23:10:25.88	+07:37:39.0	11274	45	
266	23:10:14.73	+07:39:08.6	10858	108	
269	23:10:06.28	+07:46:02.6	11775	41	
271	23:10:22.53	+07:53:25.1	15107	58	
*272	23:10:00.06	+07:35:42.9	11073	75	
N56-394		14:34:00.94	+03:44:53.4		
	250	14:33:33.52	+03:16:28.4	9190	122
	256	14:33:59.11	+03:46:40.7	8722	25
	257	14:33:58.08	+03:44:47.9	10037	19
	258	14:34:03.94	+03:44:51.2	7366	18

Table 3—Continued

Cluster	Galaxy	RA(2000)	DEC(2000)	V_H	error
	259	14:34:01.44	+03:47:50.4	8779	24
	261	14:33:55.29	+03:50:02.6	8739	24
	263	14:33:30.74	+03:41:08.3	8418	50
	264	14:33:51.41	+03:40:45.8	8702	27
	266	14:34:50.57	+03:38:41.8	8537	82
	267	14:34:08.23	+03:54:05.4	8616	22
	268	14:33:17.49	+03:54:11.9	8942	57
	269	14:33:48.30	+03:57:24.4	8810	30
	271	14:33:34.49	+03:55:52.4	25531	40
	282	14:33:38.23	+03:41:46.0	9797	35
	283	14:33:41.87	+03:41:38.0	26220	73
	284	14:33:11.88	+03:48:20.9	25784	60
	286	14:33:09.26	+03:34:29.3	9227	90
	288	14:34:05.29	+03:39:26.9	8792	131
	329	14:33:00.51	+03:47:25.7	8864	45
	*331	14:32:41.70	+03:46:30.9	8406	64
	337	14:32:49.92	+03:40:23.8	45093	97
	347	14:32:35.39	+03:16:51.8	13853	125
	*352	14:31:27.52	+03:25:03.9	16064	122
	360	14:32:21.32	+03:24:49.7	12834	78
	361	14:32:09.13	+03:25:52.3	32321	88
	*363	14:31:53.07	+03:22:47.8	1497	50
	*366	14:32:29.21	+03:27:24.3	8556	50
N03-183		07:10:50.36	+50:10:03.1		
	214	07:12:25.68	+50:39:37.1	6480	59
	227	07:12:43.63	+50:03:41.7	5487	34
	235	07:12:04.49	+50:35:31.5	5132	48
	236	07:12:03.86	+50:27:50.6	5818	95
	237	07:11:29.04	+50:40:01.7	14797	99
	238	07:11:22.59	+50:31:49.2	6206	68
	*240	07:10:35.10	+50:47:40.9	5816	50
	241	07:09:52.71	+50:27:00.3	5686	24
	247	07:11:59.72	+50:15:04.5	5777	103
	249	07:11:33.59	+50:14:53.0	6035	24
	253	07:11:04.66	+50:08:11.7	4846	39
	255	07:10:49.07	+50:14:48.3	23195	122
	257	07:10:38.62	+50:10:37.3	5648	33
	258	07:10:44.98	+50:04:52.4	5713	28
	259	07:10:34.10	+50:07:07.0	6490	23
	261	07:10:25.87	+49:56:29.9	18076	122

Table 3—Continued

Cluster	Galaxy	RA(2000)	DEC(2000)	V_H	error
	262	07:10:02.59	+50:17:41.2	18411	43
	263	07:09:42.51	+50:03:55.9	19451	122
	265	07:09:28.36	+50:09:08.4	4887	34
	266	07:11:52.00	+49:49:33.3	18621	36
	267	07:11:41.78	+49:51:43.5	6164	22
	268	07:11:37.50	+49:45:56.5	18589	47
	269	07:11:28.52	+49:33:37.8	5865	122
	270	07:11:16.31	+49:48:15.0	18398	40
	271	07:11:08.92	+49:53:59.3	6296	77
	273	07:10:53.95	+49:54:11.1	6393	19
	274	07:10:34.75	+49:52:22.2	6174	26
	275	07:09:51.01	+49:52:03.4	5427	50
	276	07:09:30.18	+49:39:11.8	18580	50
	278	07:08:38.73	+50:35:01.0	13336	119
	*279	07:08:34.23	+50:37:51.4	6164	50
	286	07:09:20.48	+50:02:48.9	18005	45
	*300	07:09:17.82	+49:52:16.1	4919	50
	*301	07:09:15.87	+49:49:12.9	4710	50
S49-140		01:56:22.89	+05:37:37.3		
	232	01:58:45.97	+05:31:30.9	6715	122
	234	01:58:46.81	+05:47:21.1	28341	56
	*253	01:57:22.60	+05:42:42.6	4263	122
	261	01:58:07.32	+05:20:16.7	31936	122
	300	01:57:03.63	+05:27:42.9	8454	113
	304	01:56:52.10	+05:46:29.0	5378	40
	309	01:56:36.80	+05:48:14.7	5655	81
	311	01:56:42.87	+05:41:16.4	5154	53
	322	01:56:19.03	+05:39:07.3	6421	76
	326	01:56:11.99	+05:35:18.6	5253	42
	326	01:56:11.99	+05:35:18.6	5349	53
	355	01:56:02.38	+05:00:04.0	9930	122
	357	01:55:27.56	+05:21:31.9	36395	122
	379	01:55:19.26	+05:27:58.6	21073	122
	385	01:54:42.42	+05:25:34.4	47490	93
	398	01:55:06.94	+05:22:24.7	5551	95
	399	01:55:02.54	+05:08:19.0	25329	108
	402	01:54:41.82	+05:05:41.0	47620	103
	405	01:53:55.53	+05:18:37.1	43495	113
S34-111		01:07:27.71	+32:23:59.7		

Table 3—Continued

Cluster	Galaxy	RA(2000)	DEC(2000)	V_H	error
	241	01:07:46.16	+32:41:34.2	5434	31
	244	01:09:42.48	+32:27:04.9	5081	56
	259	01:08:53.69	+32:30:51.9	5051	35
	261	01:08:15.85	+32:29:56.3	5661	75
	265	01:08:12.94	+32:27:12.4	4846	26
	271	01:07:24.98	+32:24:45.1	5212	28
	274	01:09:59.37	+32:22:05.8	5247	27
	286	01:09:33.28	+32:10:23.2	5606	31
	288	01:09:14.03	+32:09:04.7	4757	47
	293	01:08:55.26	+32:19:30.4	4735	59
	295	01:08:58.94	+32:14:25.8	4514	93
	296	01:08:52.33	+32:05:59.0	10617	70
	298	01:08:18.79	+32:13:35.2	5315	92
	299	01:08:43.92	+32:06:06.4	5718	87
	300	01:08:17.26	+32:05:24.1	4652	69
	304	01:07:47.17	+32:18:35.6	5534	25
	305	01:07:31.30	+32:21:42.7	5709	31
	306	01:07:33.06	+32:23:27.5	4824	33
	311	01:07:32.60	+32:05:34.0	14851	35
	318	01:09:13.50	+31:58:45.8	5255	25
	357	01:07:05.78	+32:47:42.2	5045	35
	358	01:06:51.44	+32:42:04.4	5945	48
	359	01:06:57.05	+32:37:20.3	19986	32
	360	01:07:15.68	+32:31:12.9	5492	31
	361	01:07:17.60	+32:28:58.8	4465	34
	364	01:06:53.76	+32:34:42.7	5558	116
	375	01:05:56.00	+32:24:43.7	4830	29
	391	01:07:27.22	+32:19:11.5	5156	27
	392	01:07:25.01	+32:17:33.8	4313	29
	395	01:07:11.55	+32:10:13.4	4821	52
	401	01:07:05.92	+32:20:53.0	5965	28
	402	01:06:58.21	+32:18:30.4	5581	25
S49-128		02:41:04.23	+08:43:48.5		
	248	02:41:55.63	+08:59:48.3	6103	90
	250	02:42:07.22	+08:57:08.0	21256	45
	270	02:42:45.29	+08:53:14.6	21780	64
	271	02:42:44.55	+08:50:28.7	21178	57
	276	02:42:26.84	+08:49:52.1	21296	46
	281	02:41:50.03	+08:52:45.0	6625	35
	289	02:41:16.28	+08:45:38.1	6421	90

Table 3—Continued

Cluster	Galaxy	RA(2000)	DEC(2000)	V_H	error
	290	02:41:06.12	+08:44:16.5	6365	37
	291	02:41:07.19	+08:44:06.7	6563	27
	343	02:41:53.87	+08:34:00.0	6020	27
	344	02:41:47.69	+08:23:04.6	6469	26
	346	02:41:12.81	+08:43:09.1	6044	27
	349	02:41:08.91	+08:30:09.9	20911	59
	351	02:41:10.05	+08:26:31.9	6504	27
	355	02:41:08.29	+08:12:59.1	6492	24
	406	02:40:38.30	+08:50:53.7	6097	34
	422	02:40:55.15	+08:35:44.9	5649	71
	423	02:41:01.08	+08:31:56.4	18531	125
	431	02:40:17.51	+08:43:11.0	6252	39
	440	02:39:35.97	+08:27:51.7	12340	31
MKW2		10:30:14.33	-03:12:24.2		
	234	10:30:17.36	-03:36:13.2	18340	99
	236	10:30:56.27	-03:30:34.1	11747	33
	251	10:28:03.42	-03:40:32.8	10791	16
	252	10:27:54.83	-03:33:30.2	9036	62
	253	10:28:41.82	-03:37:29.0	20925	73
	264	10:31:23.44	-03:08:01.1	12059	23
	*275	10:31:39.29	-03:16:00.5	28683	113
	281	10:31:42.92	-03:24:51.8	18444	103
	287	10:30:28.40	-03:11:43.5	11353	29
	*288	10:30:21.39	-03:05:52.6	10618	59
	291	10:30:14.60	-03:12:09.8	11346	31
	292	10:29:54.97	-03:14:07.5	11294	119
	295	10:30:14.76	-03:15:40.5	11437	28
	298	10:29:55.82	-03:20:50.3	18489	30
	305	10:29:33.90	-03:10:56.4	11628	56
	*306	10:30:57.53	-03:17:35.9	6407	81
	307	10:31:07.16	-03:14:33.4	29313	108
	*308	10:31:00.07	-03:11:05.5	12102	122
	309	10:30:41.68	-03:10:59.5	10575	40
	310	10:30:44.68	-03:10:12.8	38152	80
	317	10:30:26.03	-03:25:29.0	11554	45
	*318	10:31:06.29	-03:25:24.0	11470	113
	320	10:28:07.14	-03:16:43.5	19902	33
	321	10:28:06.80	-03:19:18.2	17844	39
	323	10:28:27.83	-03:14:34.2	10510	23
	*328	10:28:00.97	-03:20:58.9	10474	44
	329	10:27:49.78	-03:20:14.6	9033	50

Table 3—Continued

Cluster	Galaxy	RA(2000)	DEC(2000)	V_H	error
	339	10:27:36.76	-03:03:59.1	15231	31
	346	10:28:53.66	-03:15:07.3	39602	69
	348	10:29:00.22	-03:12:58.1	38045	101
	351	10:29:15.89	-03:25:37.7	13120	122
	*371	10:30:46.91	-02:45:16.9	9006	49
	373	10:30:28.90	-02:38:13.4	24727	122
	379	10:30:13.00	-02:51:37.8	29785	122
	*381	10:30:03.43	-02:49:11.3	8809	44
	383	10:29:23.80	-02:52:09.6	15222	35
	*387	10:30:46.64	-02:56:18.0	15860	44
	396	10:29:00.84	-02:57:43.9	11187	27

* Emission-Line Redshift

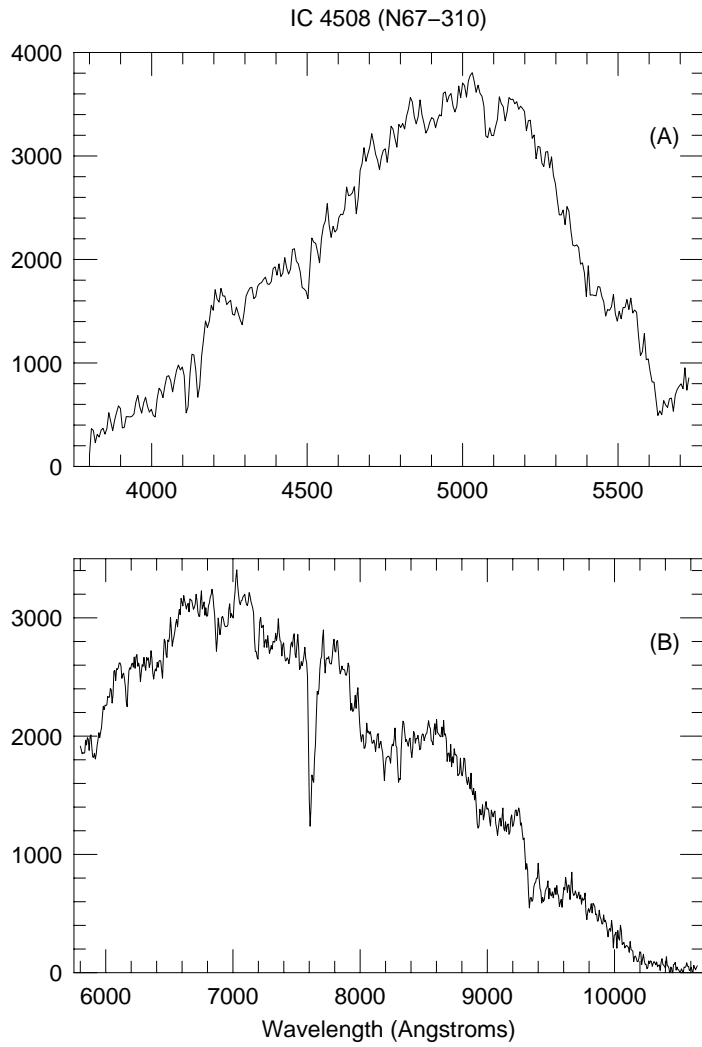


Fig. 1.— Example spectra from the ARC 3.5-m DIS spectrograph of the galaxy IC 4508 in the poor cluster N67-310. The continuum shape is distorted because of the transmission of the dichroic filter near 5750\AA . a) Blue spectrum, b) Red spectrum.

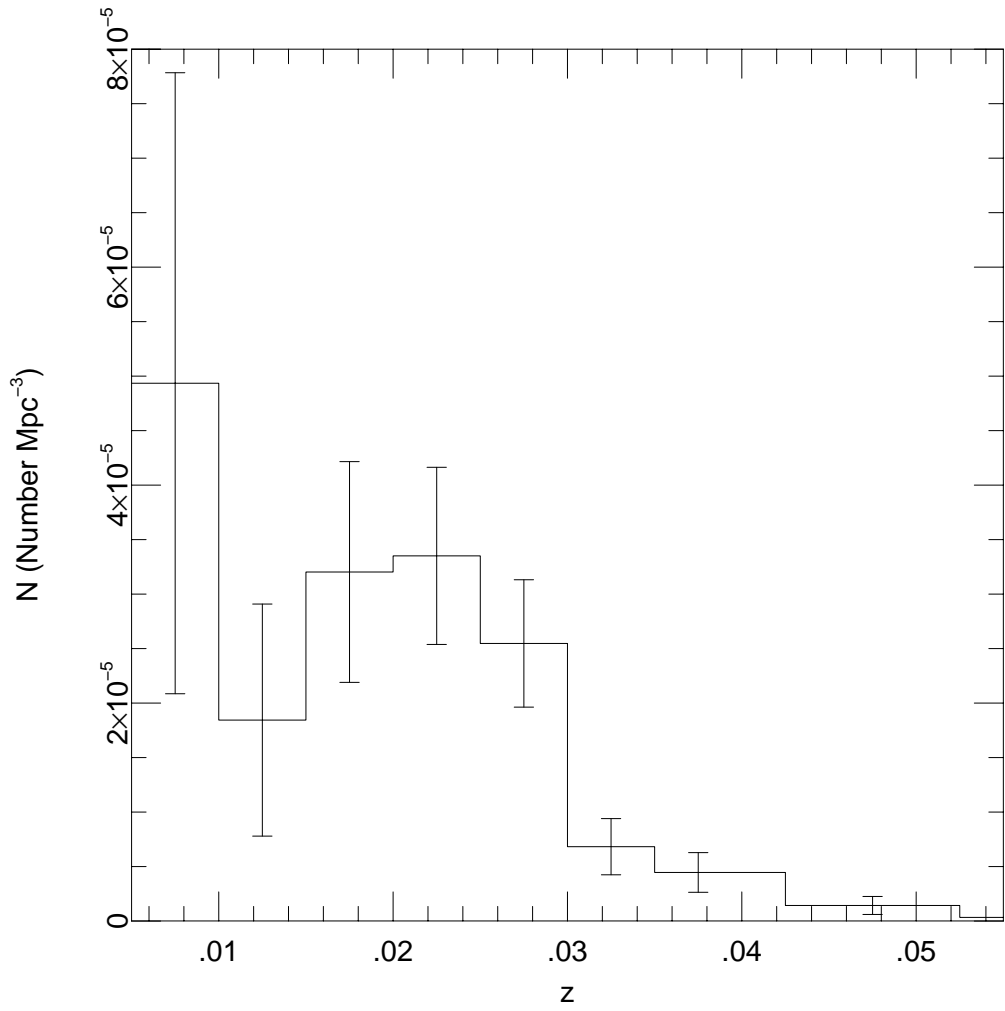


Fig. 2.— The volume-density of our poor cluster sample as a function of redshift. We judge the sample nearly complete in the redshift range $0.01 \leq z \leq 0.03$.

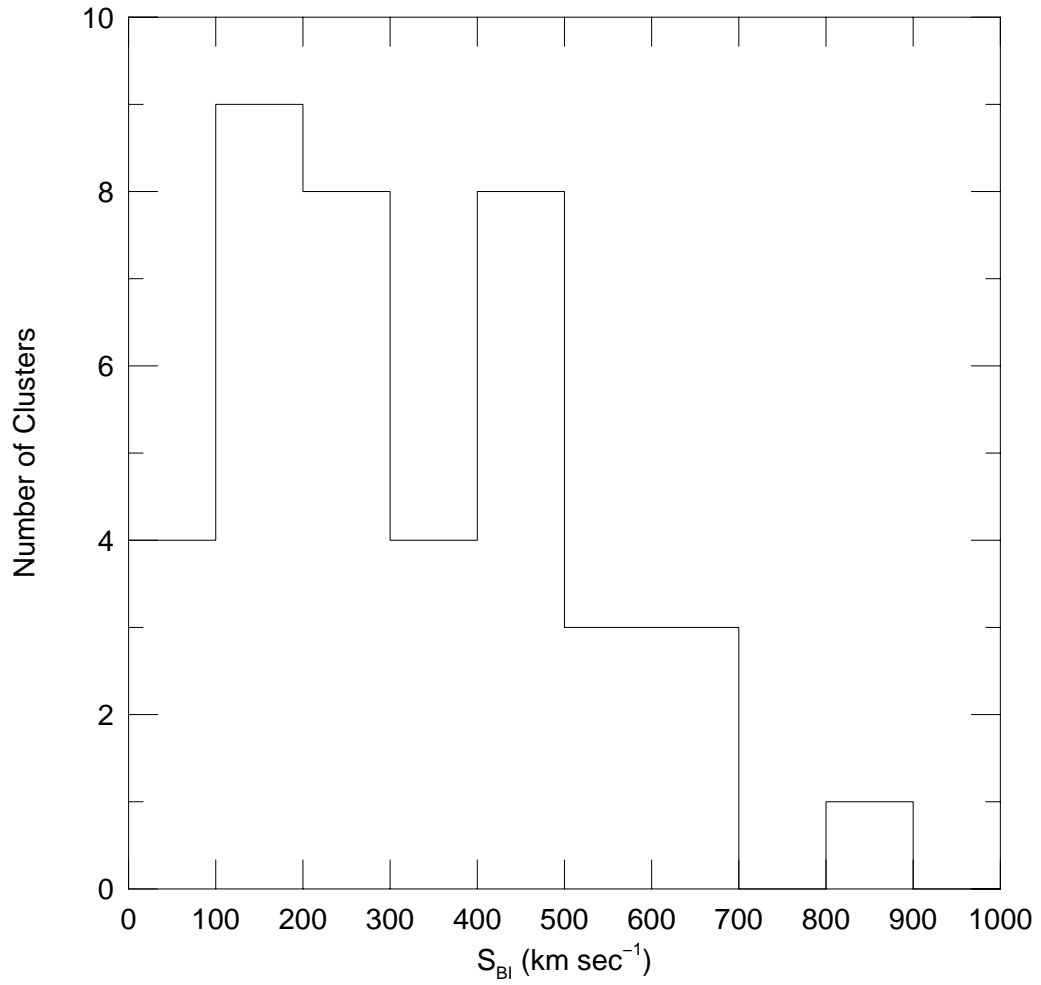


Fig. 3.— Histogram of the Biweight scale (velocity dispersion) of all poor clusters with ≥ 5 measured velocities within 0.5 Mpc of the optical cluster center.

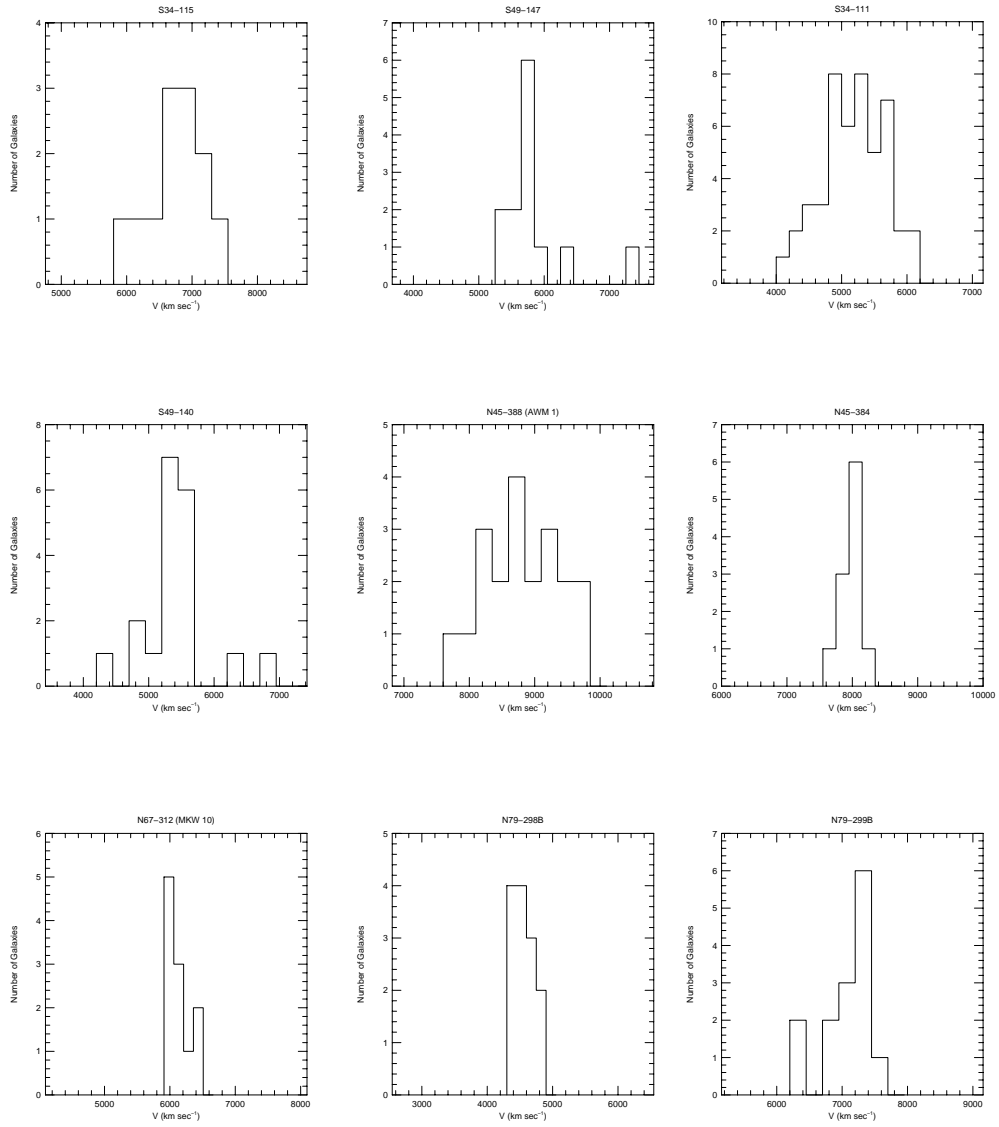
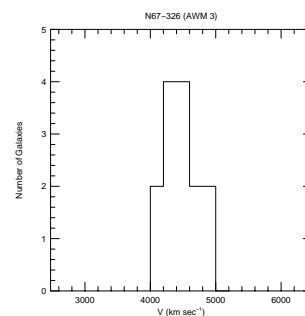
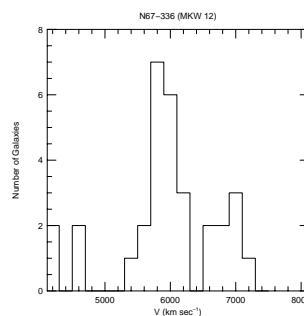
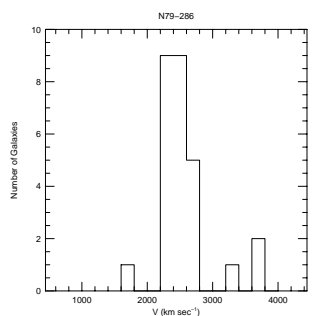
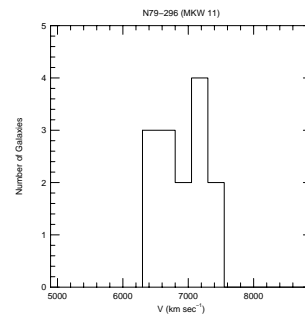
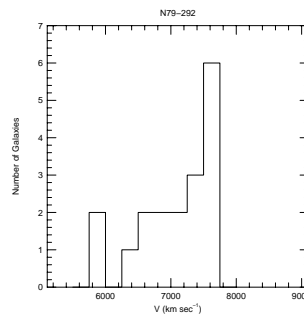
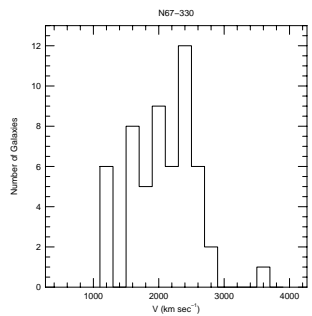
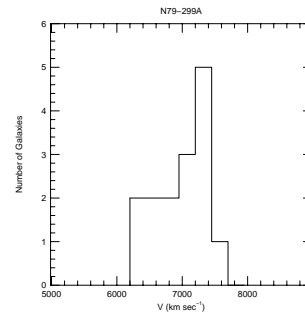
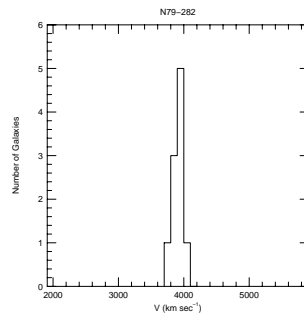
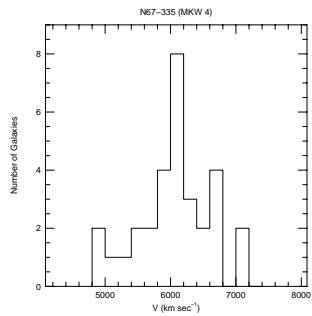
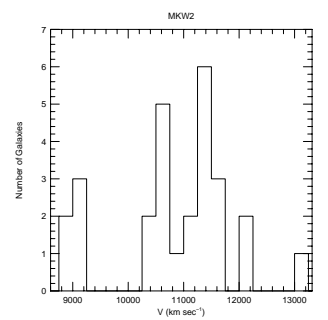
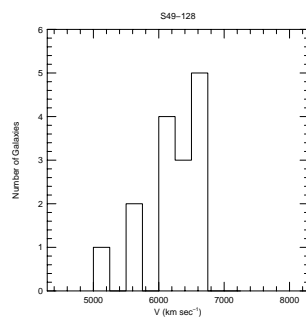
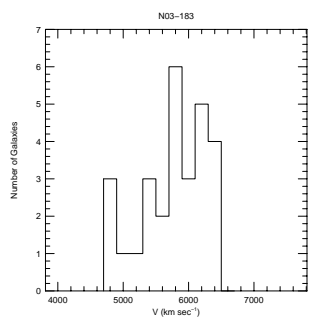
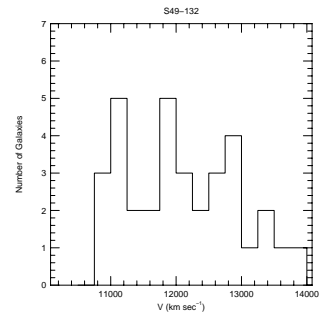
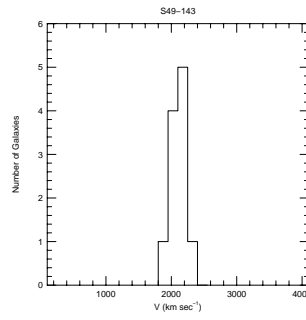
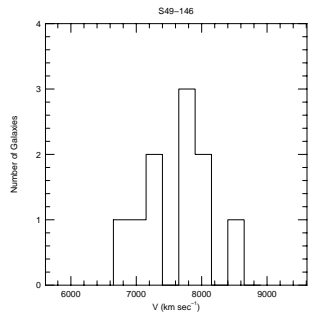
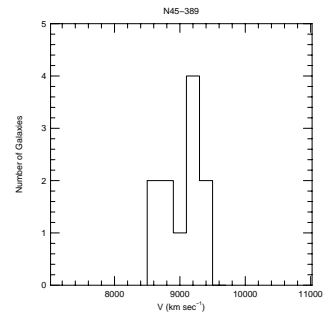
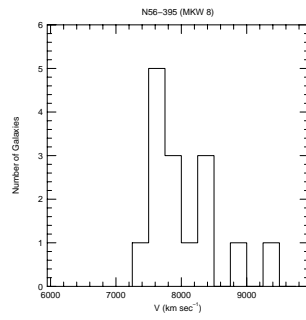
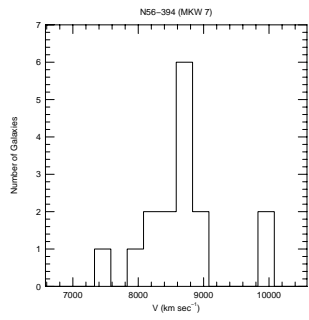


Fig. 4.— Velocity histograms for all poor clusters with ≥ 10 measured velocities. All galaxies within $1 Mpc$ and $2000 km sec^{-1}$ of the cluster mean velocity are plotted.





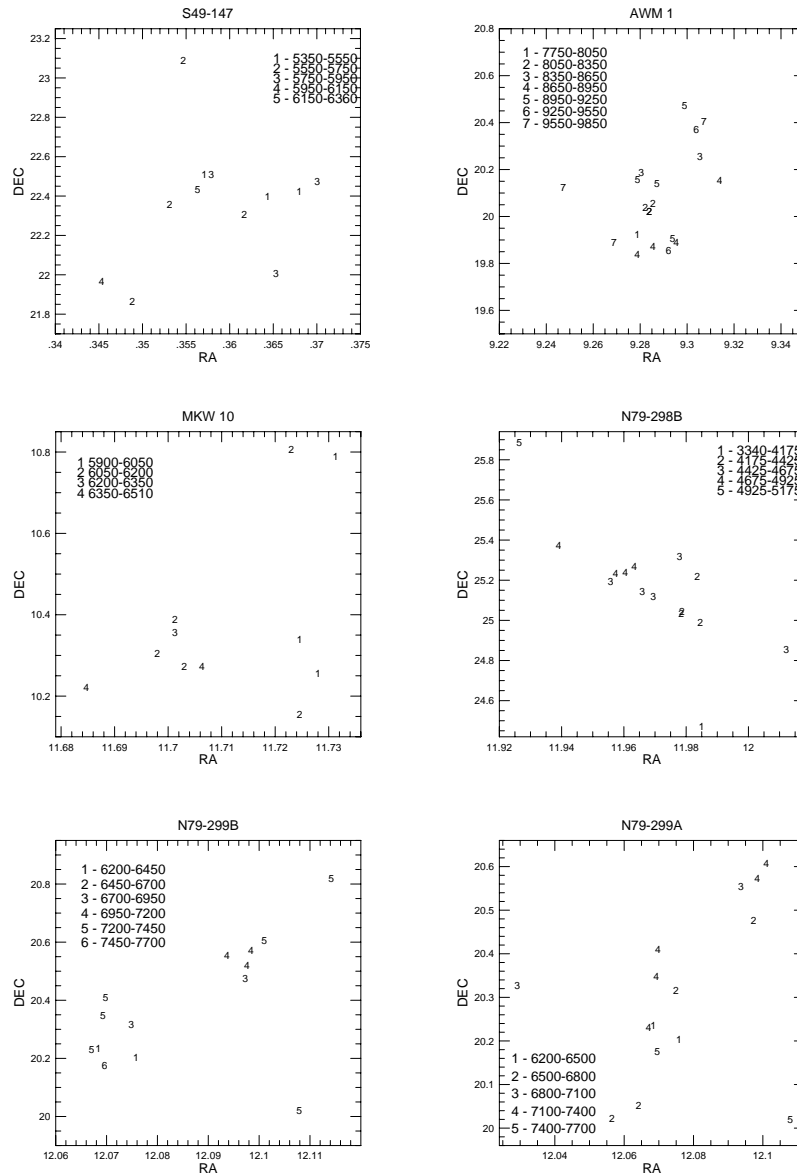


Fig. 5.— Velocity-coded diagrams of the spatial (RA and DEC) galaxy distribution for the 15 clusters with significant non-normality as determined from 1-D statistical tests. The velocity coding is labeled on the diagrams.

